Published in final edited form as:
Biochemistry. 2004 December 7; 43(48): 15276–15285.

The Δ14 Mutation of Human Cardiac Troponin T Enhances ATPase Activity and Alters the Cooperative Binding of S1-ADP to Regulated Actin†

Boris Gafurov‡, **Scott Fredricksen**‡, **Anmei Cai**‡, **Bernhard Brenner**§, **P. Bryant Chase**‖, and **Joseph M. Chalovich***,‡

Department of Biochemistry and Molecular Biology, Brody School of Medicine, East Carolina University, 600 Moye Boulevard, Greenville, North Carolina 27858-4354, Department of Molecular and Cell Physiology, Medical School Hannover, D-30623 Hannover, Germany, and Department of Biological Science and Program in Molecular Biophysics, Florida State University, Tallahassee, Florida 32306-4370

Abstract

The complex of tropomyosin and troponin binds to actin and inhibits activation of myosin ATPase activity and force production of striated muscles at low free Ca^{2+} concentrations. Ca^{2+} stimulates ATP activity, and at subsaturating actin concentrations, the binding of NEM-modified S1 to actin–tropomyosin–troponin increases the rate of ATP hydrolysis even further. We show here that the Δ14 mutation of troponin T, associated with familial hypertrophic cardiomyopathy, results in an increase in ATPase rate like that seen with wild-type troponin in the presence of NEM-S1. The enhanced ATPase activity was not due to a decreased incorporation of mutant troponin T with troponin I and troponin C to form an active troponin complex. The activating effect was more prominent with a hybrid troponin (skeletal TnI, TnC, and cardiac TnT) than with all cardiac troponin. Thus it appears that changes in the troponin–troponin contacts that result from mutations or from forming hybrids stabilize a more active state of regulated actin. An analysis of the effect of the Δ14 mutation on the equilibrium binding of S1-ADP to actin was consistent with stabilization of an active state of actin. This change in activation may be important in the development of cardiac disease.

Muscle contraction is a cyclic interaction of myosin and actin driven by the hydrolysis of ATP. Regulation of ATP hydrolysis in mammalian cardiac and skeletal muscle is mediated by four actin-associated proteins. Tropomyosin binds to seven actin monomers, and each tropomyosin is bound to a troponin complex consisting of troponin I, troponin T, and troponin C (TnI,[1] TnT, and TnC, respectively). The ATPase rate of myosin, in the presence of regulated actin, is cooperatively activated by Ca^{2+} and by ATP-free forms of myosin. The rate of ATPase activity in the absence of Ca^{2+} is low. Ca^{2+} increases the k_{cat} by ~18-fold and decreases the concentration of actin required for 50% activity by about 2-fold (*1*, *2*). The ATPase rate can be increased further (≈8-fold) by the binding of "activating" myosin (myosin–ADP, nucleotide-

†Supported by NIH Grant AR40540 (to J.M.C.), a grant from the American Heart Association (to S.F.), and NIH Grant HL63974 (to P.B.C.). A preliminary report of these data was presented at the 45th Annual Biophysical Meeting, Baltimore, MD, February 2004.

* Corresponding author. Tel: 252-744-2973. Fax: 252-744-3383. E-mail:chalovichj@mail.ecu.edu..
‡East Carolina University.
§Medical School Hannover.
‖Florida State University.

[1]Abbreviations: EDTA, ethylenediaminetetraacetic acid; EGTA, ethylene glycol bis(β-aminoethyl ether)-*N*,*N*,*N*′,*N*′-tetraacetic acid; MOPS, 3-(*N*-morpholino)propanesulfonic acid; NEM, *N*-ethylmaleimide; regulated actin, actin–tropomyosin–troponin; S1, myosin subfragment 1; SD, standard deviation; SEM, standard error of the mean; TnT, troponin T; TnI, troponin I; TnC, troponin C.

free myosin, or NEM-modified myosin) to regulated actin. This additional increase in rate appears to be due largely, if not totally, to a change in the apparent K_M for actin (3).

The effect of activating myosin binding is notable in two respects. At subsaturating actin concentrations, the ATPase rate can be greater for regulated actin than for pure actin (*4*–*7*). That is, the regulatory proteins can "potentiate" the ATPase rate as well as inhibit it (*8*). The equilibrium binding of ATP-free myosin S1 to actin is also cooperatively activated in the presence of troponin and tropomyosin (*9*, *10*). The second notable feature is that the binding of ATP-free S1 to actin can activate the ATPase rate to about the same final rate irrespective of the Ca^{2+} concentration (*3*). In the absence of Ca^{2+} a larger fraction of the regulated actin must be bound by the ATP-free myosin to reach this maximum rate. The role of the two pathways for reversing inhibition is not fully understood.

Regulation of striated muscle contraction requires the participation of tropomyosin and the three troponin components. The most enigmatic of the components has been TnT. Troponin T helps to hold the regulatory complex together by binding to tropomyosin, TnI, and TnC through its COOH half (*11*, *12*). Troponin T is also important both in potentiation of the ATPase activity (*13*) and in inhibition of ATPase activity (*14*). Troponin T has four splice variants in human heart (*15*) and two forms in bovine heart (*16*) with unique properties. Mutations in TnT also result in familial hypertrophic cardiomyopathy (*17*, *18*), dilated cardiomyopathy (*19*–*22*), and skeletal muscle nemaline myopathy (*23*). Mutations in different regions of TnT may lead to either an increase or decrease in activity (*24*, *25*). Many of the mutations leading to cardiomyopathy are in the N-terminal region or tail region of TnT. This region overlaps adjacent tropomyosin molecules and inhibits ATPase activity by stabilizing an inactive state of the actin filament. There is disagreement over the precise state that is stabilized (*14*, *26*).

We now show the effects of the Δ14 mutation of human cardiac TnT on S1 ATPase activity and on the binding of S1-ADP to actin. This mutant is missing the 14 COOH-terminal amino acids (*18*). The Δ14 mutation resulted in a higher than normal ATPase activity that was particularly noticeable at saturating Ca^{2+}. The ATPase activity at subsaturating actin but with a high NEM-S1 concentration was not significantly different from the wild type. Combining rabbit skeletal TnI and TnC with cardiac Δ14 TnT exaggerated the activating effect of the Δ14 mutation. Measurements of equilibrium binding of S1-ADP to regulated actin with the Δ14 mutation were consistent with stabilization of the active state of actin or state 2 in the Hill model (*10*). Finally, when placed into permeabilized skeletal or cardiac muscle preparations, the Δ14 mutation shifted the force–pCa relation to the left, indicating a greater ease of activation. These results support a model in which changes in the interactions among troponin subunits alter the distribution between inactive and active actin states.

MATERIALS AND METHODS

Protein Preparation

Myosin (*27*), actin (*28*, *29*), troponin, and tropomyosin (*30*) were isolated from rabbit back muscle. Myosin S1 was made by treatment of myosin with chymotrypsin (*31*). The I, T, and C components of skeletal muscle troponin were separated with a DEAE-Sephadex A-50 column equilibrated with 6 M urea, 50 mM Tris, pH 8.0, 1 mM EDTA, and 0.1 mM dithiothreitol and eluting with a gradient to 0.5 M KCl (*32*). TnI and TnT were further purified using CM-Sephadex chromatography. Bovine cardiac troponin was purified as described by Potter (*32*). All troponin components were stored at pH 6.0 at −80 °C in 6 M urea, 1 mM EDTA, 0.1 dithiothreitol, and 100 mM KCl. Troponin was reconstituted by mixing TnT, TnI, and TnC at a molar ratio of 1:1:1.5 in a buffer containing 4.5 M urea, 1 M KCl, 10 mM imidazole, pH 7, 2 mM $MgCl_2$, 50 mM $CaCl_2$, 1 mM NaN_3, and 1 mM dithiothreitol. The mixture was dialyzed against a series of similar buffers with urea concentrations of 4, 2, 1, 0.5, and 0 M

urea. The concentration of KCl was then reduced by dialysis against buffer containing 0.5 M. The final complex was checked by electrophoresis to confirm the composition ratio to be 1:1:1.

Protein concentrations were determined by light absorbance at 280 nm, corrected for scattering at 340 nm, using the following extinction coefficients ($\varepsilon^{0.1\%}$) for 280 nm: actin, 1.15; myosin S1, 0.75; tropomyosin, 0.33; troponin, 0.37.

Actin was labeled with *N*-(1-pyrenyl)iodoacetamide (*33*) and stored as a 40 μM stock in 4 mM imidazole (pH 7.0), 1 mM dithiothreitol, 2 mM $MgCl_2$, and 40 μM phalloidin. Actin was mixed with troponin and tropomyosin in a 1:1:1 molar ratio to ensure saturation of actin at the low concentrations used for binding studies. S1 was extensively modified with *N*-ethylmaleimide by incubating 4 mg/mL (A2)S1 in 50 mM Tris, pH 8, and 100 mM KCl with a 15-fold molar excess of *N*-ethylmaleimide at 25 °C for 30 min (*3*). Unreacted reagent was removed by dialysis.

Preparation of hc TnT_2 and Δ14 TnT

Human cardiac TnT_2 and the TnTΔ14 mutant lacking the C-terminal 14 amino acids from TnT_2 were subcloned in the pSBETA expression vector (*34*) and afterward expressed in *Escherichia coli*. TnT_2 is one of the four splice variants of TnT that differ in a region near the NH_2 terminus (*35*). TnT_2 has a somewhat decreased inhibitory activity than the major adult form, TnT_3 (*15*). We received the clone for human cardiac TnT_2 from Dr. Samson and used it as a template in a polymerase chain reaction (PCR) to produce hc TnT_2 cDNA suitable for subcloning in a pSBETA expression vector and to produce cDNA coding for the truncated Δ14 TnT mutant. Suitable restriction sites at either end of the cDNA were introduced by PCR, namely, *Nde*I at the 5′ end and *Bam*HI at the 3′ end. The primers used in the PCR were the 5′ primer (identical for both reactions), 5′-AGAGAGCATATGCTGACATCGAAGAGGTGGTGG-3′, and the 3′ primer for the human cardiac TnT, 5′-AGAGAGGATCCTATTTCCAGCGACCGGTGACT-3′; for the generation of the Δ14TnT mutant the 3′ primer was 5′-GAGAGGATCCTAGACTTTCTGGTTATCGTTGATCC-3′. The *Nde*I/*Bam*HI restriction enzyme-digested PCR products were purified and inserted at the same restriction sites of the pSBETA expression vector (from Dr. H.-H. Steinbiss).

The DNA sequence was confirmed using the cyclist EXO-pfu DNA sequencing kit (Stratagene) and additionally by cycle sequencing with the ABI Prism big dye terminator cycle sequencing ready reaction kit and resolving the products on an ABI Prism 377 automated sequencer (Perkin-Elmer/Applied Biosystems).

Troponin T was expressed in freshly transformed *E. coli* NovaBlue (DE3) bacteria (Novagen) and purified by modifications of published methods (*32*). The bacterial pellet was sonicated in 6 M urea, 10 mM sodium citrate, pH 7.0, 2 mM EDTA, and 1 mM dithiothreitol. Following clarification by centrifugation the supernatant was adjusted to pH 5.0. The solution was clarified again and run on a S-Sepharose column equilibrated with the same buffer. The column was eluted with a gradient of NaCl to 0.6 M. Fractions containing TnT were dialyzed four times against 6 M urea, 20 mM Tris, pH 7.8, 1 mM EDTA, and 0.3 mM dithiothreitol. The crude TnT was run on a Q-Sepharose column equilibrated in the same buffer. Following a wash the TnT was eluted with a gradient to 1 M NaCl. Fractions containing pure TnT_2 on SDS–polyacrylamide gels were used for the preparation of whole troponin. The mass of the protein product was verified by mass spectrometry at the North Carolina State University Department of Chemistry.

Equilibrium Binding Measurements

The equilibrium binding of S1-ADP to actin–tropomyosin–troponin was determined by the change in fluorescence that occurs when S1 binds to phalloidin-stabilized pyrene-labeled actin (*33*, *36*, *37*). The method used was similar to that of Tobacman and Butters (*38*). Measurements were made in a Spex Fluorolog fluorescence spectrophotometer at 25 °C with 0.5 mm slits, excitation at 364 nm, and emission at 384 nm. Each data point was the average of a 5 s data collection interval.

Binding experiments were done in a solution containing 20 mM MOPS, pH 7.0, 110 mM KCl, 5 mM $MgCl_2$, 1 mM dithiothreitol, 2 mM ADP, 0.2 mg/mL bovine serum albumin, and sufficient KCl to reach the target ionic strength and Ca-EGTA to reach the desired pCa.

The actin concentration in binding experiments was either 75 nM (at 120 mM ionic strength) or 150 nM for 180–375 mM ionic strength. Rabbit skeletal myosin S1 was used because it is well behaved in binding studies. Cardiac S1 has been reported to aggregate under some conditions (*39*). The solution also contained 14 units/mL hexokinase and 1 mM glucose to scavenge ATP and 20 μM Ap5A to inhibit ATP formation through the myokinase reaction. Ca-EGTA buffers were used to fix the free Ca^{2+} concentration (*40*). Ca^{2+}-EGTA was mixed with EGTA in ratios of 0:2, 1.4:0.6, and 2:0 mM, and the highest free Ca^{2+} concentration was obtained by using 0.1 mM $CaCl_2$ without EGTA. The free Ca^{2+} content in the solution was verified by a Corning Ca^{2+}-sensitive electrode with a Fisher Scientific AccuMet pH meter, which gave about 0, 10.3, 20, and 70 μM free Ca^{2+}, respectively.

Titrations were done by first measuring the fluorescence of a 2 mL volume of pyrene-labeled actin–tropomyosin–troponin. A small volume of a concentrated S1 stock was added to the reaction mixture in a stirred cuvette; the sample was allowed to equilibrate for at least 5 min before the fluorescence was measured. The fluorescence intensity and the concentrations of all proteins were corrected for volume changes caused by adding S1. The total volume change for an entire binding isotherm was <10%. Values of theta (ratio of S1 bound to actin total) and free S1 concentration were calculated by assuming that the fraction of actin bound was equal to the fraction of the maximum fluorescence that was achieved after the addition of S1. Additional details may be found in an earlier publication (*41*).

ATPase Rate Measurements

Rates of [^{32}P]ATP hydrolysis were determined by extracting the [^{32}P]P_i as a phosphomolybdate complex (*1*). ATPase rates were generally run in a buffer composed of 1 mM ATP, 33.8 mM KCl, 3 mM $MgCl_2$, 2 mM EGTA or 0.05 mM $CaCl_2$, 1 mM dithiothreitol, and 10 mM MOPS, pH 7. The concentration of unmodified S1 was normally 0.2 μM, and the concentration of NEM-S1 was varied to activate the actin filament. In cases where the concentration of NEM-S1 was varied, it was necessary to keep the concentration of free actin constant to avoid having the NEM-S1 act as a competitive inhibitor of the unmodified S1 ATPase activity. At the conditions of our assay virtually all of the added NEM-S1 bound to actin. Therefore, an additional amount of regulated actin equal to the concentration of NEM-S1 was added to each assay. The concentrations of tropomyosin and troponin were 0.22 and 0.15 times the actin concentration, respectively. ATPase rates were corrected for the low level of ATPase activity under the assay conditions that was due to the residual activity of the NEM-S1 [normally 0.01 μM ATP s^{-1} (μM NEM-S1)$^{-1}$].

Permeabilized Muscle Mechanics

Fiber bundles of rabbit psoas muscle were isolated, skinned with Triton X-100, equilibrated with sucrose containing skinning solution, quickly frozen in liquid propane, and stored in liquid nitrogen until use (*42*). Single fibers were isolated as described (*43*) after thawing a frozen

fiber bundle and gradually equilibrating the bundle in sucrose-free skinning solution (*42*). Detailed procedures for mechanical measurements and for exchanging foreign troponin into single rabbit fibers are given elsewhere (*44*).

Mechanical measurements with rat cardiac trabeculae were conducted as described earlier (*45*). Force–pCa relations were measured before and after exchange of the reconstituted troponin complex (sk TnC and TnI, hc TnT). Four fibers were exchanged for wild-type human cardiac TnT and two fibers for Δ14 human cardiac TnT.

Statistical Analysis and Fitting

Numerical data are presented as the mean ± standard error of the mean (SEM) when *N*, the number of measurements, was >2 or the mean ± standard deviation (SD) when $N = 2$. The Student test was used to reveal the significance of differences in measurements. Data fitting was done using either MLAB (Civilized Software, Bethesda, MD) or Sigma Plot 2000 (SSI, Richmond, CA). Coefficients predicted by the nonlinear regression in fitting procedure are presented as a coefficient ± the standard error of the regression with no *N* shown. The correlation coefficient (R^2) was usually greater than 0.96.

RESULTS

Mutations of Troponin T Enhance ATPase Activity

We examined the effect of the Δ14 mutation of human cardiac TnT_2 on ATPase activity when the TnT was complexed with bovine cardiac TnI and TnC. ATPase rates of unmodified S1 were measured with increasing concentrations of NEM-labeled S1 to test for changes in the cooperative activation of actin. NEM-S1 does not hydrolyze ATP at a high rate but does stabilize the active form of regulated actin (*46*) that we call state 2. The rates of ATP hydrolysis were corrected for the hydrolysis of ATP by NEM-S1.

The ATPase activity in the presence of wild-type troponin is shown in Figure 1A. In the absence of NEM-S1 the ATPase rate was higher in the presence of Ca^{2+} (solid circles). Increasing concentrations of NEM-S1 resulted in a further activation or potentiation (*8*) of the ATPase activity in both the presence and absence of Ca^{2+}. Less bound NEM-S1 was required to reach half of the maximum level in the presence of Ca^{2+} (1.5 ± 0.6 and 5.4 ± 1.7 μM NEM-S1, respectively), suggesting that Ca^{2+} and S1 binding synergistically activated the system. The limiting rate at high NEM-S1 concentrations was roughly the same in the absence and presence of Ca^{2+} (7.8 and 7.7 s^{-1}, respectively). Note that the limiting rates are not V_{max} values since actin concentrations were not saturating. Limiting rates represent full activation by high-affinity cross-bridges at an arbitrary actin concentration.

Figure 1B shows that substitution of the Δ14 mutant of troponin T for the wild type resulted in a 2.3-fold increase in ATPase activity compared to the wild-type case in the absence of NEM-S1 (4.5 and 2.0 s^{-1}, respectively). As in the wild type, less bound NEM-S1 was required to reach 50% of the limiting rate in the presence of Ca^{2+} (1.1 ± 0.3 and 5.8 ± 2.1 μM for Ca^{2+} and EGTA, respectively). The limiting rates at high NEM-S1 were 10.4 s^{-1} in Ca^{2+} and 8.0 s^{-1} in EGTA. The greatest effect of the mutation was in the fraction of the limiting rate that was observed in the absence of NEM-S1. In the absence of Ca^{2+} the wild-type ATPase activity was 2% of the limiting rate while the mutant activity was 3.6%. In the presence of Ca^{2+} the wild-type activity was 25% of the limiting rate while the mutant was at 43% of its limiting rate. These trends suggest that the mutation stabilized the active state of regulated actin.

We repeated a variation of this study in which the bovine cardiac TnI and TnC were replaced with the rabbit skeletal components. Figure 2A shows that the rate of ATP hydrolysis increased

with increasing NEM-S1 concentrations in both the presence and absence of Ca^{2+}. Under these conditions a plateau was reached with a rate of approximately 7/s, an increase of about 7-fold over the rate in the presence of Ca^{2+} alone (the rate at zero NEM-S1 was 14% of the limiting rate). The 50% ATPase rate levels were reached at 2.4 ± 0.7 and 5.9 ± 3.7 μM NEM-S1 in EGTA and at saturating Ca^{2+}, respectively.

Substitution of Δ14 human cardiac TnT for wild type resulted in a large increase in ATPase activity that was particularly evident in the presence of Ca^{2+}. Figure 2B shows that at zero NEM-S1 the ATPase rate in the presence of Ca^{2+} was about 7-fold higher for the mutant than for the wild type (1.0 and 7.3 s^{-1}, respectively). The rate at zero NEM-S1 for the Δ14 mutant was 80% of the limiting rate (Figure 2B). The large degree of activation was more apparent when compared to the ATPase rate of actin in the absence of troponin or tropomyosin (cross symbols). The regulatory proteins that are normally inhibitory produced an ATPase rate that was about 3 times greater than that observed with pure actin under identical conditions.

The ATPase activity of pure actin increased from 2/s to 3.2/s in going from 0 to 20 μM NEM-S1. This residual rate of 1.2/s was probably not the result of activation of pure actin but was an error introduced from the correction of ATPase rates for the rate due to NEM-S1. Errors of this magnitude occur at the highest NEM-S1 concentration in each case. We therefore consider that differences in the end point of 1–2/s are insignificant. Despite this possible source of error, experiments with wild-type troponin always exhibited ATPase rates in the absence of added NEM-S1 that were less than that of pure actin. In contrast, the ATPase activity in the case of the Δ14 mutant troponin was 3 times that of pure actin.

A trivial explanation for any observed effect resulting from a mutation in troponin T is that the troponin T could no longer form a complex with troponin I and troponin C. When mixed with actin and tropomyosin, the troponin complex formed with Δ14 TnT had a normal composition. To determine if the mutant troponin T was functioning when complexed with TnI and TnC, we compared the activity of this complex with the binary complex of TnI and TnC. Figure 3 shows that the ATPase activity in the presence of rabbit skeletal TnI-TnC was different from that seen with Δ14 TnT-TnI-TnC. The absence of troponin T led to a low level of activation by Ca^{2+} alone that was quite distinct from that seen with the Δ14 mutation of troponin T. The pattern in the absence of troponin T more closely resembled whole troponin containing wild-type troponin T. These results indicate that Δ14 TnT-TnI-TnC was functional but the function was modified by the mutation.

Table 1 summarizes the rates for zero NEM-S1 ± Ca^{2+} and gives the percent of total activation (defined by the limiting rate at high NEM-S1 concentrations) that was achieved by the addition of Ca^{2+} alone. Ca^{2+} alone produced only 11% of the limiting rate in the absence of TnT. Wild-type human cardiac TnT2 and rabbit skeletal TnT increased the activation in Ca^{2+} to 14% when combined with rabbit skeletal TnI and TnC (although the activity in EGTA was greater for human cardiac TnT_2). Wild-type human cardiac TnT_2 produced 25% of the limiting rate when combined with bovine cardiac TnI and TnC. Values of the limiting rate from 43% to 80% occurred when Δ14 TnT_2 was present. These results confirm the activating effect of TnT (*13*).

A possible cause of the large activation of ATPase activity in the case of Δ14 TnT is that the mutation stabilized an active form of regulated actin. We investigated this possibility by measuring the fraction of S1-ADP bound to the regulated actin with increasing S1-ADP concentrations as done earlier (*9*, *10*). Although both S1-ADP and rigor S1 are activating, the affinity of S1-ADP for actin is lower and more readily measured.

Measurements of equilibrium binding of S1-ADP were made at six different ionic strengths ranging from 120 to 375 mM. Each ionic strength curve was repeated three to six times.

Whenever possible, actin concentrations were kept well below the dissociation constant to permit accurate determination of the free S1-ADP concentration. The binding affinity at 120 mM ionic strength was sufficiently high that data collection was difficult even at 75 nM actin. At higher ionic strengths the actin concentration was either 75 or 150 nM.

Figure 4 shows examples (120, 180, 225, and 260 mM ionic strength) of isotherms for binding of S1-ADP to regulated actin as a function of the free S1-ADP concentration in the presence of 2 mM EGTA. Paired studies were done with troponin formed from either human cardiac wild type or Δ14 TnT and bovine cardiac TnI and TnC. Binding in the presence of the Δ14 mutant exhibited small but reproducible differences from the wild type. In general, the mutant tended to make a transition to the higher affinity state, state 2 (*10*), more readily.

Cooperative binding as in Figure 4 can be analyzed in terms of the Hill model (*10*) having two major states of regulated actin. The binding curves are described by four parameters. K_1 and K_2 are the affinities of S1-ADP for the low- and high-affinity states of actin, respectively. L' is the equilibrium constant (inactive state/active state) for transition of the entire actin filament but without bound S1. L' should not be confused with a related parameter L, the constant for an isolated actin–tropomyosin–troponin unit with no neighbors, no bound Ca^{2+}, and no bound S1. Y is the cooperativity parameter; large values of Y mean that adjacent regulatory units tend to be in the same state. Parameters determined from fitting the Hill model to data were insensitive to K_1 but dependent on the other parameters.

In fitting the Hill model to the data, the value of Y can be constrained to values that give positive cooperativity ($Y > 1$) or allowed to include both negative and positive cooperative effects ($Y > 0$). The data could be fitted very well with either assumption, but the values of L' were dependent on constraints to Y. We analyzed the data for both cases. Figure 5 contains plots of the log of L', Y, and K_2 as a function of the square root of ionic strength for wild-type and Δ14 mutant troponin. When the value of Y was not constrained, the value of L' increased with increasing ionic strength for both wild-type and mutant troponin (Figure 5A). Values of L' were lower for the mutant troponin at all ionic strengths, indicating that the inactive state of actin was destabilized. Values of Y (Figure 5B) and K_2 (Figure 5C) decreased with increasing ionic strength in a similar manner for wild-type and Δ14 troponin.

If Y was constrained to prohibit negative cooperativity, the ionic strength dependence of L' was attenuated but the values for the wild type remained higher than those for the Δ14 mutant (Figure 5D). Values of Y decreased with increasing ionic strength but leveled off at 1, indicating the absence of cooperativity (Figure 5E). Values of K_2 decreased with increasing ionic strength; the slope was about the same as with the fit with unrestricted values of Y (Figure 5F).

Figure 5 also includes earlier parameters obtained for the binding of S1 to actin in the presence of rabbit skeletal troponin–tropomyosin in which the troponin was isolated as an intact complex (*41*). The values of K_2 are indistinguishable from both the wild-type and mutant cardiac troponin. Y' was less sensitive to ionic strength for the skeletal troponin. Values of L' increased with ionic strength similarly to the cardiac troponin. However, the values of L' were higher than the wild-type cardiac troponin.

The Δ14 mutation of troponin T affected the equilibrium binding of S1-ADP to regulated actin in the presence of free Ca^{2+} as well as in the absence of free Ca^{2+}. We measured S1-ADP binding at three additional free Ca^{2+} concentrations (10, 20, and 70 μM). Figure 6 shows S1-ADP binding to regulated actin having either wild-type or Δ14 troponin T at 180 mM ionic strength at 10 μM free Ca^{2+} concentration. Although only the 10 μM Ca^{2+} case is shown in the figure, the fitted curves are a global fit of data collected at all four Ca^{2+} concentrations. A global fit was possible because the values of L, K_1, and K_2 are not Ca^{2+} dependent. An expanded view of the initial parts of the binding curves is shown in the inset. Binding in the presence of

Ca^{2+} was less sigmoidal presumably because of a decreased population of actin in the inhibited state. Differences were observed between the wild type and the Δ14 mutant at all Ca^{2+} concentrations.

Figure 7 gives the Ca^{2+} dependence of binding parameters L' and Y with the constraint that $Y > 1$ (only positive cooperativity permitted). The value of L' decreased with increasing free Ca^{2+}, but the values of L' were lower for the Δ14 mutant at all free Ca^{2+} concentrations. The cooperativity parameter, Y, increased with increasing Ca^{2+} concentrations in both cases. At this ionic strength Y was lower in the case of the mutant but only in the absence of Ca^{2+}. This means that the interaction between adjacent cooperative units was not greatly affected by the mutation. The Δ14 mutant troponin also produced small increases in both K_2 (3.1×10^6 M^{-1} compared to 2.4×10^6 M^{-1}) and L (11 and 9.9). However, the only substantial difference produced by the mutation was a change in L' that suggests that actin filaments containing the mutant troponin shift more readily to the active state.

Values of L', Y, and K_2 were also calculated with the assumption that $Y > 0$ (positive and negative cooperativity). The results of this case are not shown because the only values that changed were those of the Δ14 mutant in EGTA. In that case, Y was reduced from 1 to 0.45, L' was decreased from 3.6 to 3.1, and K_2 increased from 2.9×10^6 to 3.1×10^6 M^{-1}.

The Δ14 mutation affects the force–pCa relationship in both skeletal and cardiac muscle preparations. We measured the effect of the Δ14 mutation in skinned skeletal and cardiac muscle fibers using our exchange method to replace the troponin in skinned muscle preparations (*44*, *45*). The troponin used was a hybrid of either wild-type human cardiac TnT or the Δ14 mutant with rabbit skeletal TnI and TnC. Figure 8 shows the normalized force of skeletal muscle fibers as a function of the pCa. Fibers reconstituted with Δ14 troponin were activated at lower Ca^{2+} concentrations than with wild-type TnT by 0.3 pCa unit. Prior to exchange the pCa was 5.6. Following exchange with wild-type human cardiac TnT–rabbit skeletal TnI–TnC the pCa was reduced to 5.5. When exchanged with Δ14 TnT the pCa was 5.9. Exchanging the rabbit skeletal TnT with human cardiac TnT reduced the Hill coefficient in the skeletal fibers from 4.7 to 1.7, but that value was unaffected by the Δ14 mutation.

In permeabilized cardiac trabeculae preparations, maximum force was measured at pCa 5 before and after passive exchange of troponin in seven preparations exchanged with troponin containing TnT-Δ14 and in seven additional preparations exchanged with wild-type troponin. The maximum force of wild-type-exchanged trabeculae was 61 + 6 ($N = 7$) of the preexchange force. The maximum force of mutant troponin-exchanged trabeculae was 62 ± 6 ($N = 7$) of the preexchange force and was not significantly different ($P > 0.05$) from that for wild type. Figure 9 shows that the change in pCa_{50} for trabeculae following exchange with wild-type troponin was 0.00 ± 0.02 pCa unit ($N = 4$). Following exchange with mutant troponin the change in pCa_{50} was 0.18 ± 0.03 pCa unit ($N = 5$), i.e., in the direction of increased Ca^{2+} sensitivity. Comparison of postexchange force–pCa data shows that the human cardiac TnTΔ14 mutant increased Ca^{2+} sensitivity of isometric force generation of cardiac myofilaments by approximately 0.2 pCa (Figure 9).

Activation of steady-state isometric force in both cardiac and skeletal preparations occurred at a lower free Ca^{2+} concentration when troponin T was replaced with the Δ14 mutant form. This change in Ca^{2+} sensitivity supports the concept that activation is facilitated under isometric as well as unloaded conditions of ATPase assays, by a mutation that is associated with cardiac disease.

DISCUSSION

We show evidence here that deletion of part of the COOH-terminal region of TnT, as seen in some cases of familial hypertrophic cardiomyopathy, results in stabilization of regulated actin in a more active state. This conclusion was based on elevated ATPase rates, on similar rates of ATPase activity at high concentrations of NEM-S1, and on parameters derived from equilibrium binding studies. Isomeric force studies on cardiac and skeletal muscle preparations were consistent with this interpretation. We suggest that stabilization of the active state of actin resulted from a change in troponin–troponin interactions resulting from the mutation. Thus the effect of the TnT mutation depended on the source of the other troponin subunits. Skeletal muscle TnI and TnC complexed with Δ14 cardiac TnT produced a more extreme case than found with all cardiac troponin.

We found it advantageous to use skeletal muscle actin, tropomyosin, and S1 in this study because of our body of data using these proteins (*41*). Accurate measurements may be made with skeletal S1 because it does not tend to aggregate. Because identical experiments were run with Δ14 and wild-type TnT, all changes could be attributed to the mutation. The source of actin, tropomyosin, and S1 did not appear to have a significant impact on the results since similar effects were observed when mutant troponin was placed into cardiac and skeletal muscle fibers.

We were able to acquire the TnT_2 isoform for the present study. The isoforms of TnT used in earlier studies were not always identified. Isoform variations occur near the NH_2 region of the TnT and are far removed from the region of the Δ14 mutation. Because our wild type and mutant were both derived from the TnT_2 form, the changes that we have observed are due to changes in the COOH-terminal region. Nevertheless, we cannot rule out that the magnitude of the effects reported here could differ with other TnT isoforms.

Another factor that could influence the properties of the troponin complex is the process of refolding the isolated TnI, TnT, and TnT into a functioning troponin complex. We found that the fraction of soluble troponin obtained from a reconstitution was greater when done with skeletal TnI-TnC than with human cardiac TnI-TnC. Yet the potentiation of ATPase activity was greater for the cardiac–skeletal hybrid. Thus, the activation observed with the Δ14 mutation in cardiac troponin cannot be attributed to improper reconstitution.

Just as we observed the Δ14 mutant of TnT to stabilize the active state of actin, Nakaura et al. observed an increased activity of muscle fibers having the Δ14 TnT mutant (*47*). Substitution of 28 residues from the C-terminus of TnT with 7 other residues in transgenic mice also produced hypersensitivity to Ca^{2+} and impaired diastolic function (*48*). That same mutant resulted in decreased cooperativity of skeletal muscle S1-ADP binding to skeletal muscle actin–cardiac muscle tropomyosin in EGTA at 180 mM ionic strength (*49*). Like the result presented here this is consistent with a facilitated transition to a more active state of actin. On the other hand, Mukherjea et al. observed reduced activation of ATPase in Ca^{2+} in the presence of the Δ14 TnT mutant (*50*). In general, mutations of TnT tend to be activating rather than inhibiting. Among the effects reported for various mutations are an increased Ca^{2+} sensitivity (*50–56*), increased ATPase activity (*53*, *55*, *57*), decreased inhibition (*54*), and increased shortening velocity (*58*).

Incorporation of Δ14 TnT into troponin did not merely increase the ATPase activity relative to wild-type troponin but produced rates that, in the presence of Ca^{2+}, exceeded those measured in the absence of regulatory proteins. This suggests that the troponin–tropomyosin complex modifies the catalytic activity of actin. This potentiation of activity occurs with other mutations associated with familial hypertrophic cardiomyopathy including those in TnI and tropomyosin. Mutations K206Q, K183Δ, and G203S in cardiac TnI increase both the maximum sliding speed

and the Ca^{2+} sensitivity of regulated filament sliding in in vitro motility assays (*45*). Mutations V95A, D175N, and E180G in α-tropomyosin increase Ca^{2+} sensitivity of filament sliding in motility assays (*6*, *59*). Furthermore, the potentiation of activity is also sensitive to the type of actin (Acanthamoeba > rabbit skeletal) (*4*) and tropomyosin (smooth > skeletal) (*7*). Phosphorylation of TnI can also produce activities greater than those observed with pure actin (*60*). Tropomyosin–troponin may also increase the maximum filament sliding speed in motility assays (*61*). Because this elevated activity may arise by several types of changes, it is likely that in all cases actin is ultimately altered so that its k_{cat}/K_M is increased. Other data also support the idea that actin may have multiple conformations (*62*, *63*) and thus multiple activities.

The activity of regulated actin at any condition is determined by the distribution of actin states. The distribution of states is dictated by numerous protein–protein contacts among the components of the actin filament. Regulated actin is mostly in the inactive state in the absence of bound Ca^{2+}, S1-ADP, or S1. Under these conditions TnI binds to actin and stabilizes tropomyosin in an inactive state. The physical link between tropomyosin and TnI is TnT. The COOH-terminal region of TnT is important for binding to TnI (*64*,*65*). Deletion of the extreme COOH-terminal region of TnT weakens the binding to TnI (*50*). A reduction in coupling between tropomyosin and TnI might easily stabilize the active state as we have observed here. Mutations in TnT may be particularly suited to alter actin filament distributions since troponin T is important in activating ATPase rates (*13*, *66*). Stabilization of the active state was more extreme when rabbit skeletal TnI and TnC were complexed with human cardiac TnT. Relatively small structural changes retard the ability of troponin to keep tropomyosin in the inhibitory position.

The model of Hill et al. (*10*) was used here because this model can simulate potentiation and inhibition of ATPase (*67*) as well as equilibrium binding and binding kinetics (*41*,*68*, *69*). The decrease in L' seen with the Δ14 mutant of TnT may be interpreted as stabilization of a more active state of actin. If analyzed by the model of McKillop and Geeves, this would be equivalent to an increase in K_T (*70*). It is likely that other models can simulate the binding data in this paper. However, models based on blocking of S1-ATP binding by troponin–tropomyosin cannot explain the enhancement of activity except to suggest that tropomyosin can also enhance the binding of S1-ATP to actin. This also implies an allosteric change in actin. The ATPase and equilibrium binding data shown here as well as our earlier data (*41*) provide challenging tests of models of regulation.

Our earlier studies with rabbit skeletal troponin showed that the parameters L' and Y change with ionic strength (*41*). We wished to ensure that the effects seen with the mutation were not restricted to some narrow range of conditions. The binding of S1-ADP to regulated actin was examined from 120 to 375 mM ionic strength. Analysis with the Hill model showed that K_2 was the same for wild type and Δ14 TnT. Values of the cooperativity parameter, Y, were similar for the wild type and Δ14 mutant over that same range of conditions. The value of L' was consistently decreased for the Δ14 mutation, indicating stabilization of the active state of regulated actin over the range of conditions.

The ionic strength dependencies of the equilibrium binding parameters for cardiac troponin were similar to those measured earlier for skeletal troponin (*41*). Values of L' increased and values of Y and K_2 decreased with increasing ionic strength. In the absence of Ca^{2+} skeletal muscle troponin favors the inactive state more than does cardiac troponin, and the transition to the active state tends to be more positively cooperative.

Because changes in the state of actin can either increase or decrease the activity of the thin filament and because the stability of each state is dictated by the interactions of several proteins, it is reasonable that changes in the distribution of actin states are common in disease causing

mutations. However, not every mutation may result in a change in the cooperative transition between actin states. Two mutations of bovine cardiac tropomyosin (A63V and K70T) that produce an increase in Ca^{2+} sensitivity of ATPase activity did not alter the equilibrium binding of skeletal S1 to skeletal actin (*71*). It will be interesting to see how many other mutations in TnT and TnI result in changes in either the distribution of actin states or the kinetics of the transition among these states.

Acknowledgements

We thank Ms. Amanda Clark for assistance with cardiac muscle mechanics, Mr. Michael Vy-Freedman for help with protein preparations, and Dr. Mechthild Schroeter for critical reading of the manuscript.

References

1. Chalovich JM, Eisenberg E. Inhibition of actomyosin ATPase activity by troponin-tropomyosin without blocking the binding of myosin to actin. J Biol Chem 1982;257:2432–2437. [PubMed: 6460759]
2. El-Saleh SC, Potter JD. Calcium-insensitive binding of heavy meromyosin to regulated actin at physiological ionic strength. J Biol Chem 1985;260:14775–14779. [PubMed: 2932449]
3. Williams DL Jr, Greene LE, Eisenberg E. Cooperative turning on of myosin subfragment 1 adenosine triphosphatase activity by the troponin-tropomyosin-actin complex. Biochemistry 1988;27:6987–6993. [PubMed: 2973810]
4. Eisenberg E, Weihing RR. Effect of skeletal muscle native tropomyosin on the interaction of amoeba actin with heavy meromyosin. Nature 1970;228:1092–1093. [PubMed: 4249428]
5. Murray JM, Knox MK, Trueblood CE, Weber A. Potentiated state of the tropomyosin actin filament and nucleotide-containing myosin subfragment 1. Biochemistry 1982;21:906–915. [PubMed: 6462176]
6. Lehrer SS, Morris EP. Dual effects of tropomyosin and troponin-tropomyosin on actomyosin subfragment 1 ATPase. J Biol Chem 1982;257:8073–8080. [PubMed: 6123507]
7. Sobieszek A. Steady-state kinetic studies on the actin activation of skeletal muscle heavy meromyosin subfragments. J Mol Biol 1982;157:275–286. [PubMed: 6213786]
8. Bremel RD, Murray JM, Weber A. Manifestations of cooperative behavior in the regulated actin filament during actin-activated ATP hydrolysis in the presence of calcium. Cold Spring Harbor Symp Quant Biol 1972;37:267–275.
9. Greene LE, Eisenberg E. Cooperative binding of myosin subfragment-1 to the actin-troponin-tropomyosin complex. Proc Natl Acad Sci USA 1980;77:2616–2620. [PubMed: 6930656]
10. Hill TL, Eisenberg E, Greene LE. Theoretical model for the cooperative equilibrium binding of myosin sub-fragment 1 to the actin-troponin-tropomyosin complex. Proc Natl Acad Sci USA 1980;77:3186–3190. [PubMed: 10627230]
11. Zot AS, Potter JD. Structural aspects of troponin-tropomyosin regulation of skeletal muscle contraction. Annu Rev Biophys Biophys Chem 1987;16:535–539. [PubMed: 2954560]
12. Perry SV. Troponin T: Genetics, properties and function. J Muscle Res Cell Motil 1998;19:575–602. [PubMed: 9742444]
13. Potter JD, Sheng Z, Pan BS, Zhao J. A direct regulatory role for troponin T and a dual role for troponin C in the Ca^{2+} regulation of muscle contraction. J Biol Chem 1995;270:2557–2562. [PubMed: 7852318]
14. Tobacman LS, Nihli M, Butters C, Heller M, Hatch V, Craig R, Lehman W, Homsher E. The troponin tail domain promotes a conformational state of the thin filament that suppresses myosin activity. J Biol Chem 2002;277:27636–27642. [PubMed: 12011043]
15. Gomes AV, Guzman G, Zhao J, Potter JD. Cardiac troponin T isoforms affect the Ca2+ sensitivity and inhibition of force development. Insights into the role of troponin T isoforms in the heart. J Biol Chem 2003;277:35341–35349. [PubMed: 12093807]
16. Tobacman LS, Lee R. Isolation and functional comparison of bovine cardiac troponin T isoforms. J Biol Chem 1987;262:4059–4064. [PubMed: 2951382]

17. Watkins H, McKenna WJ, Thierfelder L, Suk HJ, Anan R, O'Donoghue A, Spirito P, Matsumori A, Moravec CS, Seidman JG, Seidman CE. Mutations in the genes for cardiac troponin T and α-tropomyosin in hypertrophic cardiomyopathy. N Engl J Med 1995;332:1058–1064. [PubMed: 7898523]

18. Thierfelder L, Watkins H, MacRae C, Lamas R, McKenna W, Vosberg HP, Seidman JG, Seidman CE. α-Tropomyosin and cardiac troponin T mutations cause familial hypertrophic cardiomyopathy: A disease of the sarcomere. Cell 1994;77:701–712. [PubMed: 8205619]

19. Biesiadecki BJ, Jin JP. Exon skipping in cardiac troponin T of turkeys with inherited dilated cardiomyopathy. J Biol Chem 2002;277:18459–18468. [PubMed: 11886865]

20. Fujino N, Shimizu M, Ino H, Yamaguchi M, Yasuda T, Nagata M, Konno T, Mabuchi H. A novel mutation Lys273Glu in the cardiac troponin T gene shows high degree of penetrance and transition from hypertrophic to dilated cardiomyopathy. Am J Cardiol 2002;89:29–33. [PubMed: 11779518]

21. Morimoto S, Lu QW, Harada K, Takahashi-Yanaga F, Minakami R, Ohta M, Sasaguri T, Ohtsuki I. Ca^{2+} -desensitizing effect of a deletion mutation DeltaK210 in cardiac troponin T that causes familial dilated cardiomyopathy. Proc Natl Acad Sci USA 2002;99:913–918. [PubMed: 11773635]

22. Robinson P, Mirza M, Knott A, Abdulrazzak H, Willott R, Marston S, Watkins H, Redwood C. Alterations in thin filament regulation induced by a human cardiac troponin T mutant that causes dilated cardiomyopathy are distinct from those induced by troponin T mutants that cause hypertrophic cardiomyopathy. J Biol Chem 2002;277:40710–40716. [PubMed: 12186860]

23. Johnston JJ, Kelley RI, Crawford TOMDH, Agarwala R, Koch T, Schaffer AA, Francomano CA, Biesecker LG. A novel nemaline myopathy in the Amish caused by a mutation in troponin T1. Am J Hum Genet 2000;67:814–821. [PubMed: 10952871]

24. Tobacman LS, Lin D, Butters C, Landis C, Back N, Pavlov D, Homsher E. Functional consequences of troponin T mutations found in hypertrophic cardiomyopathy. J Biol Chem 1999;274:28363–28370. [PubMed: 10497196]

25. Knollmann BC, Potter JD. Altered regulation of cardiac muscle contraction by troponin T mutations that cause familial hypertrophic cardiomyopathy. Trends Cardiovasc Med 2001;11:206–212. [PubMed: 11597833]

26. Maytum R, Geeves MA, Lehrer SS. A modulatory role for the troponin T tail domain in thin filament regulation. J Biol Chem 2002;277:29774–29780. [PubMed: 12045197]

27. Kielley WW, Harrington WF. A model for the myosin molecule. Biochim Biophys Acta 1960;41:401–421. [PubMed: 14408979]

28. Spudich JA, Watt S. The regulation of rabbit skeletal muscle contraction. I. Biochemical studies of the interaction of the tropomyosin-troponin complex with actin and the proteolytic fragments of myosin. J Biol Chem 1971;246:4866–4871. [PubMed: 4254541]

29. Eisenberg E, Kielley WW. Evidence for a refractory state of heavy meromyosin and subfragment-1 unable to bind to actin in the presence of ATP. Cold Spring Harbor Symp Quant Biol 1972;37:145–152.

30. Eisenberg E, Kielley WW. Troponin-tropomyosin complex. Column chromatographic separation and activity of the three active troponin components with and without tropomyosin present. J Biol Chem 1974;249:4742–4748. [PubMed: 4276966]

31. Weeds AG, Taylor RS. Separation of subfragment-1 isozymes from rabbit skeletal muscle myosin. Nature 1975;257:54–56. [PubMed: 125854]

32. Potter JD. Preparation of troponin and its subunits. Methods Enzymol 1982;85:241–263. [PubMed: 7121270]

33. Kouyama T, Mihashi K. Fluorimetry study of *N*-(1-pyrenyl)iodoacetamide-labeled F-actin: local structural change of actin protomer both on polymerization and on binding of heavy meromyosin. Eur J Biochem 1981;114:33–38. [PubMed: 7011802]

34. Schenk PM, Baumann S, Mattes R, Steinbiss HH. Improved high-level expression system for eukaryotic genes in *Escherichia coli* using T7 RNA polymerase and rare Arg tRNAs. BioTechniques 1995;19:196–200. [PubMed: 8527135]

35. Marston SB, Redwood CS. Modulation of thin filament activation by breakdown or isoform switching of thin filament proteins—Physiological and pathological implications. Circ Res 2003;93:1170–1178. [PubMed: 14670832]

36. Dancker P, Low I, Hasselbach W, Wieland T. Interaction of actin with phalloidin: polymerization and stabilization of F-actin. Biochim Biophys Acta 1975;400:407–414. [PubMed: 126084]
37. Criddle AH, Geeves MA, Jeffries T. The use of actin labeled with *N*-(1-pyrenyl)iodoacetamide to study the interaction of actin with myosin subfragments and troponin/tropomyosin. Biochem J 1985;232:343–349. [PubMed: 3911945]
38. Tobacman LS, Butters CA. A new model of cooperative myosin-thin filament binding. J Biol Chem 2000;275:27587–27593. [PubMed: 10864931]
39. Flamig DP, Cusanovich MA. Aggregation-linked kinetic heterogeneity in bovine cardiac myosin subfragment 1. Biochemistry 1981;20:6760–6767. [PubMed: 7317351]
40. Fabiato A, Fabiato F. Calculator programs for computing the composition of the solutions containing multiple metals and ligands used for experiments in skinned muscle cells. J Physiol (Paris) 1979;75:463–505. [PubMed: 533865]
41. Gafurov, B., Chen, Y. D., and Chalovich, J. M. (2004) Ca^{2+} and ionic strength dependencies of S1-ADP binding to actin-tropomyosin-troponin: regulatory implications, Biophys. J. (in press).
42. Kraft T, Chalovich JM, Yu LC, Brenner B. Parallel inhibition of active force and relaxed fiber stiffness by caldesmon fragments at physiological ionic strength and temperature conditions: Additional evidence that weak cross-bridge binding to actin is an essential intermediate for force generation. Biophys J 1995;68:2404–2418. [PubMed: 7647245]
43. Yu LC, Brenner B. Structures of actomyosin crossbridges in relaxed and rigor muscle fibers. Biophys J 1989;55:441–453. [PubMed: 2930830]
44. Brenner B, Kraft T, Yu LC, Chalovich JM. Thin filament activation probed by fluorescence of *N*-((2-(iodoacetoxy)ethyl)-*N*-methyl)amino-7-nitrobenz-2-oxa-1,3-diazole-labeled troponin I incorporated into skinned fibers of rabbit psoas muscle. Biophys J 1999;77:2677–2691. [PubMed: 10545368]
45. Köhler J, Chen Y, Brenner B, Gordon AM, Kraft T, Martyn DA, Regnier M, Rivera AJ, Wang CK, Chase PB. Familial hypertrophic cardiomyopathy mutations in troponin I (K183Δ, G203S, K206Q) enhance filament sliding. Physiol Genomics 2003;14:117–128. [PubMed: 12759477]
46. Pemrick S, Weber A. Mechanism of inhibition of relaxation by *N*-ethylmaleimide treatment of myosin. Biochemistry 1976;15:5193–5198. [PubMed: 136272]
47. Nakaura H, Morimoto S, Yanaga F, Nakata M, Nishi H, Imaizumi T, Ohtsuki I. Functional changes in troponin T by a splice donor site mutation that causes hypertrophic cardiomyopathy. Am J Physiol Cell Physiol 1999;277:C225–C232.
48. Tardiff JC, Factor SM, Tompkins BD, Hewett TE, Palmer BM, Moore RL, Schwartz S, Robbins J, Leinwand LA. A truncated cardiac troponin T molecule in transgenic mice suggests multiple cellular mechanisms for familial hypertrophic cardiomyopathy. J Clin Invest 1998;101:2800–2811. [PubMed: 9637714]
49. Burhop J, Rosol M, Craig R, Tobacman LS, Lehman W. Effects of a cardiomyopathy-causing troponin T mutation on thin filament function and structure. J Biol Chem 2001;276:20788–20794. [PubMed: 11262409]
50. Mukherjea P, Tong L, Seidman JG, Seidman CE, Hitchcock-DeGregori SE. Altered regulatory function of two familial hypertrophic cardiomyopathy troponin T mutants. Biochemistry 1999;38:13296–13301. [PubMed: 10529204]
51. Harada K, Takahashi-Yanaga F, Minakami R, Morimoto S, Ohtsuki I. Functional consequences of the deletion mutation DeltaGlu160 in human cardiac troponin T. J Biochem (Tokyo) 2000;127:263–268. [PubMed: 10731693]
52. Nakaura H, Yanaga F, Ohtsuki I, Morimoto S. Effects of missense mutations Phe110Ile and Glu244Asp in human cardiac troponin T on force generation in skinned cardiac muscle fibers. J Biochem (Tokyo) 1999;126:457–460. [PubMed: 10467159]
53. Szczesna D, Zhang R, Zhao JJ, Jones M, Guzman G, Potter JD. Altered regulation of cardiac muscle contraction by troponin T mutations that cause familial hypertrophic cardiomyopathy. J Biol Chem 2000;275:624–630. [PubMed: 10617660]
54. Redwood C, Lohmann K, Bing W, Esposito GM, Elliott K, Abdulrazzak H, Knott A, Purcell I, Marston S, Watkins H. Investigation of a truncated cardiac troponin T that causes familial hypertrophic cardiomyopathy—Ca^{2+} regulatory properties of reconstituted thin filaments depend on the ratio of mutant to wild-type protein. Circ Res 2000;86:1146–1152. [PubMed: 10850966]

55. Yanaga F, Morimoto S, Ohtsuki I. Ca^{2+} sensitization and potentiation of the maximum level of myofibrillar ATPase activity caused by mutations of troponin T found in familial hypertrophic cardiomyopathy. J Biol Chem 1999;274:8806–8812. [PubMed: 10085122]
56. Morimoto S, Yanaga F, Minakami R, Ohtsuki I. Ca^{2+}-sensitizing effects of the mutations at Ile-79 and Arg-92 of troponin T in hypertrophic cardiomyopathy. Am J Physiol Cell Physiol 1998;275:C200–C207.
57. Takahashi-Yanaga F, Ohtsuki I, Morimoto S. Effects of troponin T mutations in familial hypertrophic cardiomyopathy on regulatory functions of other troponin subunits. J Biochem (Tokyo) 2001;130:127–131. [PubMed: 11432788]
58. Lin D, Bobkova A, Homsher E, Tobacman LS. Altered cardiac troponin T in vitro function in the presence of a mutation implicated in familial hypertrophic cardiomyopathy. J Clin Invest 1996;97:2842–2848. [PubMed: 8675696]
59. Wang F, Grubich JR, Chase PB. Familial hypertrophic cardiomyopathy mutations in alpha-tropomyosin enhance actin filament sliding at sub-saturating [Ca^{2+}]. J Mol Cell Cardiol 2003;35:A30.
60. Deng Y, Schmidtmann A, Kruse S, Filatov V, Heilmeyer LMG Jr, Jaquet K, Thieleczek R. Phosphorylation of human cardiac troponin I G203S and K206Q linked to familial hypertrophic cardiomyopathy affects actomyosin interaction in different ways. J Mol Cell Cardiol 2003;35:1365–1374. [PubMed: 14596793]
61. Gordon AM, LaMadrid MA, Chen Y, Luo Z, Chase PB. Calcium regulation of skeletal muscle thin filament motility in vitro. Biophys J 1997;72:1295–1307. [PubMed: 9138575]
62. Homsher E, Nili M, Chen IY, Tobacman LS. Regulatory proteins alter nucleotide binding to actomyosin of sliding filaments in motility assays. Biophys J 2003;85:1046–1052. [PubMed: 12885651]
63. Egelman EH. Actin allostery again? Nat Struct Biol 2001;8:735–736. [PubMed: 11524667]
64. Takeda S, Yamashita A, Maeda K, Maéda Y. Structure of the core domain of human cardiac troponin in the Ca^{2+}-saturated form. Nature 2003;424:35–41. [PubMed: 12840750]
65. Malnic B, Farah CS, Reinach FC. Regulatory properties of the NH2- and COOH-terminal domains of troponin T—ATPase activation and binding to troponin I and troponin C. J Biol Chem 1998;273:10594–10601. [PubMed: 9553120]
66. Bing W, Fraser IDC, Marston SB. Troponin I and troponin T interact with troponin C to produce different Ca^{2+}-dependent effects on actin-tropomyosin filament motility. Biochem J 1997;327:335–340. [PubMed: 9359398]
67. Hill TL, Eisenberg E, Chalovich JM. Theoretical models for cooperative steady-state ATPase activity of myosin subfragment-1 on regulated actin. Biophys J 1981;35:99–112. [PubMed: 6455170]
68. Brenner B, Chalovich JM. Kinetics of thin filament activation probed by fluorescence of *N*-((2-(iodoacetoxy)ethyl)-*N*-methyl)amino-7-nitrobenz-2-oxa-1,3-diazole-labeled troponin I incorporated into skinned fibers of rabbit psoas muscle: implications for regulation of muscle contraction. Biophys J 1999;77:2692–2708. [PubMed: 10545369]
69. Chen Y, Yan B, Chalovich JM, Brenner B. Theoretical kinetic studies of models for binding myosin sub-fragment-1 to regulated actin: Hill model versus Geeves model. Biophys J 2001;80:2338–2349. [PubMed: 11325734]
70. Maytum R, Lehrer SS, Geeves MA. Cooperativity and switching within the three-state model of muscle regulation. Biochemistry 1999;38:1102–1110. [PubMed: 9894007]
71. Heller MJ, Nili M, Homsher E, Tobacman LS. Cardiomyopathic tropomyosin mutations that increase thin filament Ca^{2+} sensitivity and tropomyosin N-domain flexibility. J Biol Chem 2003;278:41742–41748. [PubMed: 12900417]

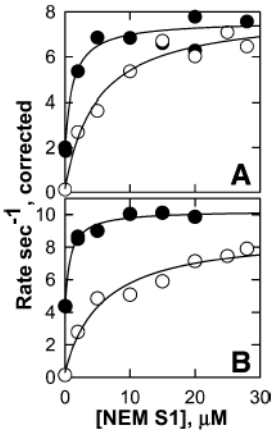

Figure 1.

Actin-activated ATPase activity of S1 with increasing binding of activating cross-bridges, NEM-S1. The ATPase rate was corrected for S1 alone and for the hydrolysis by NEM-S1 [the residual activity of NEM-S1 was normally 0.01 μM ATP s^{-1} (μM NEM-S1)$^{-1}$]. (A) ATPase rates in the presence of wild-type human cardiac TnT_2 reconstituted with bovine cardiac TnI and TnC. The initial rates at NEM − S1 = 0 were 2.0 ± 0.14 and 0.15 ± 0.028 s^{-1} (N = 2) in Ca or EGTA, respectively. (B) ATP rates in the presence of the Δ14 TnT mutant reconstituted with bovine cardiac TnI and TnC. The initial rates were 4.5 ± 0.24 and 0.19 ± 0.01 s^{-1} (N = 3). Symbols: solid, Ca^{2+}; open, EGTA. Conditions: 1 mM ATP, 3 mM $MgCl_2$, 10 mM MOPS, pH 7.0, 34 mM KCl, 1 mM dithiothreitol, 10 μM actin, 2.2 μM tropomyosin, and 0.2 μM S1.

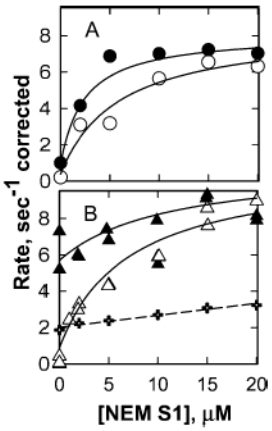

Figure 2.

Actin-activated ATPase activity as a function of the concentration of NEM-S1. The ATPase rate was corrected for S1 alone and for the hydrolysis by NEM-S1. (A) Wild-type human cardiac TnT_2 reconstituted with rabbit skeletal TnI and TnC. The initial rates were 1.0 ± 0.07 and 0.2 ± 0.03 s^{-1} ($N = 3$) in Ca or EGTA, respectively. (B) Δ14 TnT mutant reconstituted with rabbit skeletal TnI and TnC. The initial rates were 7.3 ± 0.54 and 0.41 ± 0.06 s^{-1} ($N = 4$). The crosses are a control for actin with no regulatory proteins to demonstrate the potentiation of ATPase activity. Symbols: solid, Ca^{2+}; open, EGTA. Conditions: 1 mM ATP, 3 mM $MgCl_2$, 10 mM imidazole, pH 7.0, 34 mM KCl, 1 mM dithiothreitol, 10 μM actin, 2.2 μM tropomyosin, and 0.2 μM S1.

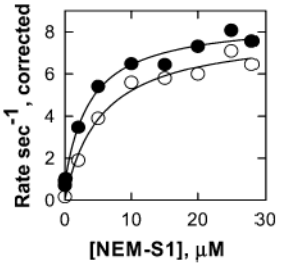

Figure 3.

Control ATPase rate measured when the troponin construct had rabbit skeletal TnI and TnC only. ATP rates in the presence of rabbit skeletal TnI, TnC, and skeletal tropomyosin (neither human cardiac nor Δ14 mutant TnT_2 was used). Note that the absence of TnT does not lead to potentiation. Therefore, the mutants (Figures 1B and 2B) do not act by simply preventing TnT binding. The initial rates were 0.84 ± 0.1 and 0.22 ± 0.07 s^{-1} ($N = 3$) in Ca^{2+} or EGTA, respectively. Symbols: solid, Ca^{2+}; open, EGTA.

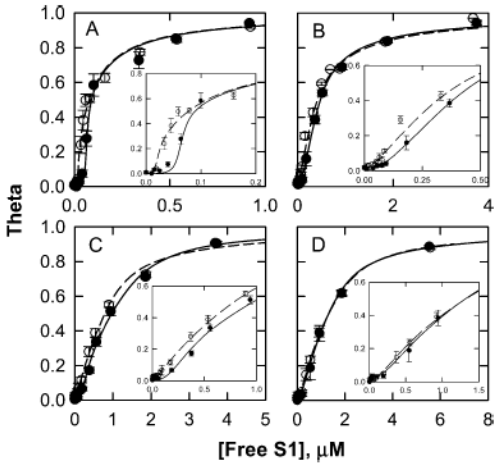

Figure 4.

Equilibrium isotherms of S1·ADP binding to actin–tropomyosin–troponin at different ionic strengths in Ca^{2+}-free solution: (A) 120, (B) 180, (C) 225, and (D) 260 mM ionic strength. Ionic strengths of 300 and 375 mM were not shown because the difference between WT and Δ14 mutant troponin T became negligible. Points are averages of three to six measurements, bars show the SEM, and lines are curve fits. Open circles and dashed lines represent binding isotherms and Hill's model fit, respectively, obtained for the Δ14 troponin T mutant at a given ionic strength. Closed circles and solid lines show results obtained with WT troponin. Parameters from analyses of these data are given in Figure 5. Inserts on each panel show the magnified beginning portion of the binding isotherm.

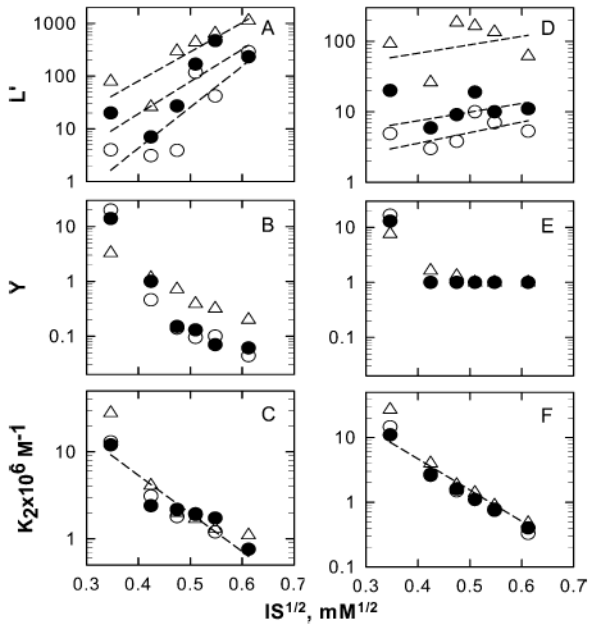

Figure 5.

Dependences of equilibrium binding parameters from the Hill model on the square root of the ionic strength at 2 mM EGTA. (A) and (D) show L', the equilibrium constant for transition between states for the entire actin filament with Ca^{2+} but without S1. (B) and (E) show the cooperativity parameter, Y. (C) and (F) show the affinity of S1-ADP for actin in the active state, state 2. Curves in (A) – (C) were generated with the constraint $Y > 0$ (both negative and positive cooperativity possible). Curves in (D) – (F) were generated by constraining $Y \geq 1$. Note that all ordinates are on a log scale. Symbols: (○) Δ14 TnT mutant, (•) WT TnT, (Δ) rabbit skeletal troponin–tropomyosin (from ref 41).

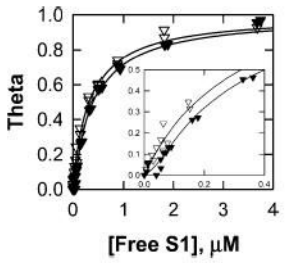

Figure 6.
Equilibrium isotherms of S1 binding to regulated actin at 10 μM free Ca^{2+} and 180 mM ionic strength in the presence of either the Δ14 mutant or wild-type troponin. Solid lines show Hill model fits to WT troponin (▼) or the Δ14 mutant (▽). Inset: initial part of binding curve. Fit parameters are shown in Figure 7.

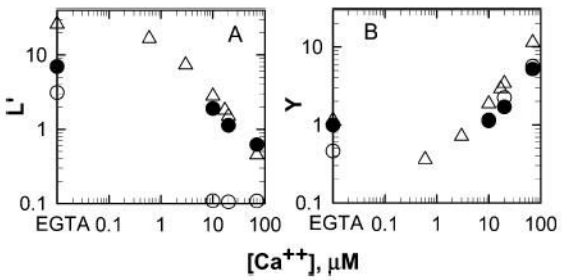

Figure 7.

Calcium dependence of the Hill model parameters for equilibrium binding of S1 to regulated actin at 180 mM ionic strength. (A) L' is the equilibrium constant for transition between states for the entire actin filament with Ca^{2+} but without S1. (B) Y is the cooperativity parameter. K_2, the binding constant, and L, the equilibrium constant for transition between states of an isolated actin unit, were 3.1×10^6 M^{-1} and 11 for the Δ14 mutant troponin and 2.4×10^6 M K_1, and K_2 are not Ca [1] and 9.9 for WT troponin. Symbols: (○) Δ14 TnT mutant; (•) WT TnT; (Δ) rabbit skeletal tropomyosin–troponin from ref 41. Note that both axes are on a log scale.

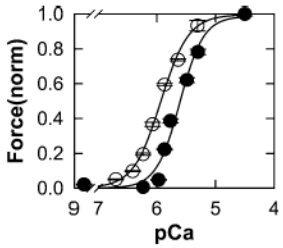

Figure 8.

Force production measured in skinned muscle fibers from rabbit skeletal muscle. The plot shows normalized isometric steady-state force production of a fiber before exchange (solid circles) and after exchange with troponin containing Δ14 mutant TnT (open circles). Error bars show the SEM. Solid lines are the theoretical curves obtained by fitting the data to $1/(1 + 10^{(pCa-pCa_{50})n})$, where n is the Hill cooperativity parameter. Preexchange: $pCa_{50} = 5.6 \pm 0.05$, $n = 4.7 \pm 0.5$, and $R^2 = 0.99$ (two fibers). Exchanged with the Δ14 mutant: $pCa_{50} = 5.9 \pm 0.01$, $n = 1.8 \pm 0.1$, and $R^2 = 0.99$ (two fibers). Exchanged with wild-type human cardiac TnT, rabbit skeletal TnI, and TnC: $pCa_{50} = 5.5 \pm 0.1$, $n = 1.7 \pm 0.4$, and $R^2 = 0.99$ (four fibers). The latter curve is not shown.

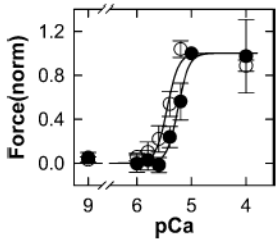

Figure 9.

Force production measured in skinned trabeculae from rat cardiac muscle. The graph shows isometric steady-state force production in the presence of wild-type troponin (solid circles) and Δ14 mutant TnT (open circles). Error bars show the SEM. Steady-state force was normalized by subtracting passive force measured in the initial pCa = 9 solution to obtain active force and then dividing the resulting force at each pCa by the active force at pCa = 5. Solid lines are theoretical curves obtained by fitting the equation given in Figure 8 to the data. Exchanged with troponin containing wild-type human cardiac TnT: $pCa_{50} = 5.25 \pm 0.02$, $n = 4.3 \pm 0.7$, and $R^2 = 0.99$. Exchanged with troponin containing Δ14 mutant TnT: $pCa_{50} = 5.45 \pm 0.03$, $n = 4.2 \pm 1.0$, and $R^2 = 0.97$. The temperature was 15 °C.

Table 1

Summary of the Effects of Different Troponin Types on ATPase Rates

TnT	TnI	TnC	ATPase rate at min NEM-S1		% max in Ca^{2+}
			EGTA	Ca^{2+}	
rs[a]	rs	rs	0.1	1.1	14
none	rs	rs	0.22	0.84	11
hc TnT_2	rs	rs	0.2	1.0	14
hc R92Q	rs	rs	0.27	3.2	45
hc Δ14	rs	rs	0.41	7.3	80
hc TnT_2	bc	bc	0.15	2.0	25
hc Δ14	bc	bc	0.19	4.5	43

[a]Figures are not shown for rabbit skeletal troponin. TnT, TnI, and TnC were from rabbit skeletal (rs), human cardiac (hc), and bovine cardiac (bc) sources.